JOURNAL OF CATALYSIS **158,** 109–115 (1996)
ARTICLE NO. 0012

Study of Cs-Promoted, α-Alumina-Supported Silver Ethylene-Epoxidation Catalysts

I. Characterization of the Support and As-Prepared Catalyst

David M. Minahan* and Gar. B. Hoflund†

Union Carbide Corporation, Technical Center/P.O. Box 8361, South Charleston, West Virginia 25303; and †Department of Chemical Engineering, University of Florida, Gainesville, Florida 32611

Received May 9, 1995; revised September 6, 1995; accepted September 11, 1995

An α-alumina support and a Cs-promoted Ag/α-Al_2O_3 ethylene-epoxidation catalyst prepared on this same support have been characterized using secondary electron microscopy (SEM), electron dispersive X-ray spectroscopy (EDS), ion scattering spectroscopy (ISS), Auger electron spectroscopy (AES), and X-ray photoelectron spectroscopy (XPS). The SEM micrographs indicate that the α-alumina is crystalline with a well-defined plane exposed and that the Ag covers the support surface uniformly as a thin film. The EDS data also support the assertion that both surfaces are fairly uniform with regard to composition. ISS data exhibit features due to many contaminants such as C, N, Ca, and Ni on the α-alumina, as well as Na and Si binder materials which are also observed with AES and XPS. The XPS chemical-state data for the O, Al, Na, C, and Ag are complex, indicating that multiple chemical states of each element are present. Apparently, Ag is present predominantly as AgO, but Ag_2O and Ag metal are also present. © 1996 Academic Press, Inc.

INTRODUCTION

Ethylene oxide production is a large-volume business. In the United States, 6.78 billion lbs. was produced in 1994, placing it at 26th in capacity on the list of manufactured chemicals (1). Of this, 6.1 billion lbs. was converted by hydrolysis to ethylene glycol (30th on the list) which is used for antifreeze in automobile cooling systems or to make polyester fibers. Ethylene oxide is produced commercially exclusively by the partial oxidation of ethylene, using air or oxygen, over a heterogeneous catalyst based on the original concept by Lefort (2) in 1931. The major problem is that a fraction of the ethylene is combusted to CO_2 and H_2O. Although the separation processes are not difficult, valuable feedstock is wasted by combustion. Silver supported on low surface area α-alumina and promoted with an alkali metal is the only catalyst used commercially to selectively oxidize ethylene to ethylene oxide. Industrial operating selectivities are normally close to 80% compared to about 68% during the 1960s. Much of this improvement is due to the addition of alkali promoters (3). The commercial operating conditions are dictated by the explosion limits for the inlet gas containing ethylene and oxygen; i.e., the reaction is run in an oxygen-limited regime. Conversion per pass ranges from 20 to 40% so gas recycle is employed. Typical operating temperatures are 230 to 280°C at pressures from 150 to 450 psi for a contact period of about 1 s (4). Chlorine-containing compounds are added continuously to the feed in very small quantities as moderators.

These catalysts are extremely complex, and very little is understood fundamentally about how they function. Many surface characterization studies have been carried out on the oxygen/silver system (single crystal or polycrystalline surfaces) in order to gain information which may relate to ethylene epoxidation catalysts, and many kinetic studies have been carried out on alumina-supported Ag catalysts. An excellent review of the studies published before 1987 has been presented by Van Santen and Kuipers (5). The state of the silver is often assumed to be metallic, but high surface oxygen concentrations are required to give optimal catalytic performance and metallic silver behaves quite differently than alumina-supported silver for ethylene epoxidation. The α-alumina is inert and nonacidic to minimize ethylene oxide isomerization and combustion. A large pore size is necessary to minimize diffusional limitations which would reduce selectivity. This fact limits the surface area of these catalysts to about 1 m^2/g because higher surface areas at the same pore size would yield catalysts of low pill integrity which would powder with time and plug the reactor tubes.

Results of characterization studies using surface analytical techniques to examine alumina-supported Ag epoxidation catalysts have not been published previously. This paper is the first in a series which reports results obtained on these catalysts using techniques including X-ray photo-

0021-9517/96 $12.00
Copyright © 1996 by Academic Press, Inc.
All rights of reproduction in any form reserved.

electron spectroscopy (XPS), Auger electron spectroscopy (AES), ion scattering spectroscopy (ISS), scanning electron microscopy (SEM), and electron dispersive X-ray spectroscopy (EDS). Information has been gained about catalyst preparation, aging behavior, and the influence of a Cs promotor. The catalytic reaction data obtained from this catalyst is presented in the next part of this study (6).

Each of the techniques utilized provides a particular but different type of information about this complex industrial catalyst. The information is complimentary and when combined yields a detailed understanding of the morphology, composition and chemical nature of α-alumina-supported Ag. ISS, AES, and XPS provide compositional information with varying surface sensitivities. ISS is highly surface sensitive detecting atoms in the outermost layer only. This technique has been discussed in a review by Miller (7) and a series of papers by Young and co-workers (8–11). AES and XPS are much less surface sensitive than ISS generally probing 40 to 60 Å beneath the surface depending upon the kinetic energies of the electrons being detected and the experimental geometry. For this reason and the fact that the surfaces are rough and highly nonhomogeneous, compositions cannot be calculated from the AES and XPS data. The importance of the matrix effect (elemental distribution within the near-surface region) has been demonstrated in an angle-resolved AES study by Hoflund *et al.* (12). High-resolution XPS data provide chemical-state information about the elements present in the near-surface region. SEM provides micrographs which are important with regard to visualizing morphology and interpreting the ISS, AES, and XPS data. EDS yields high spatial resolution compositional information, but it probes deeply beneath the surface due to the high kinetic energy of the primary beam and the fact that X-rays are detected.

EXPERIMENTAL

Catalyst Preparation

The Cs-promoted, α-alumina supported Ag catalyst was prepared by impregnation based on a patent by Bhasin *et al.* (13). An 88 wt% lactic acid solution was heated to 75°C, and a CsOH solution was added while stirring. Then Ag_2O powder was added to the lactic acid solution while stirring to dissolve the suspended matter. A commercial α-alumina support ($\frac{1}{8}''$ extrudate) with a 1.3 m^2/g surface area and purity of 99.6% (the rest is a Na- and Si-containing binder material) was impregnated with the lactic acid solution at 80°C for 15 min. The solution was allowed to drain for 1 h, and the pellets were calcined at 500°C in air on a belt roaster. The resulting catalyst contains 13.87 wt% Ag and 420 ppm by weight Cs.

Characterization Details

For characterization studies the catalyst pellets were physically ground in a mortar and pestle which had been ultrasonically cleaned in soap water, distilled water, toluene, acetone, trichoroethylene, acetone and ethanol. Previous studies have shown that these pellets fragment to expose the catalytically active surface area within the pores and that grinding does not affect the nature of the active surface. The powder was then pressed into pellet form in an Al cup. This sample was then attached to a stainless steel sample holder and inserted into the ultrahigh vacuum system (base pressure $<1 \times 10^{-10}$ Torr) for surface characterization with XPS, AES, and ISS. These data were collected using a double-pass cylindrical mirror analyzer (CMA, Perkin–Elmer PHI Model 25-270AR) equipped with an internal electron gun. For XPS, the X rays were generated using a PHI Model 04-151 single Mg anode $K\alpha$ source with an energy of 1253.6 eV and FWHM of 0.7 eV. The CMA was operated in the retarding mode using pass energies of 25 eV to collect high-resolution spectra and 50 eV to collect survey spectra. The data were collected using a computer-interfaced digital pulse counter (14) and smoothed numerically (15). AES was performed by operating the CMA in the nonretarding mode and using a primary beam energy of 3 keV. The conventional experimental geometry (12, 16) was used to collect the AES data. Phase-sensitive detection was used with a 0.5 V_{pp}, 10 kHz sine wave applied to the outer cylinder of the CMA. ISS data were collected using the CMA in the nonretarding mode, pulse counting detection, a scattering angle of 148° and 1 keV He^+. The 100 nA ion beam was defocused over an area of 5 mm diameter, and an ISS spectrum was collected in 90 s. The experimental conditions used for AES and ISS result in minimal sample alteration.

RESULTS AND DISCUSSION

SEM/EDS

SEM micrographs obtained from the α-alumina support and the Cs-promoted Ag/α-Al_2O_3 catalyst are shown in Figs. 1a and 1b, respectively. The bare α-alumina appears to be rather structureless, but it is actually crystalline with a very flat planar surface exposed. Careful inspection reveals information about the crystalline structure and the presence of terraced layers leading up to the exposed plane. Some small (0.1 to 1 μm) nearly spherical particles are also apparent which may be comprised of the Na and Si binder material or Al_4C_3 formed from burnout material used to control pore size during support preparation. The micrograph taken from the catalyst shows that the alumina support appears to be quite uniformly coated with a thin film of Ag. The planar α-alumina structure can be observed at some points in the micrograph, but the α-alumina is

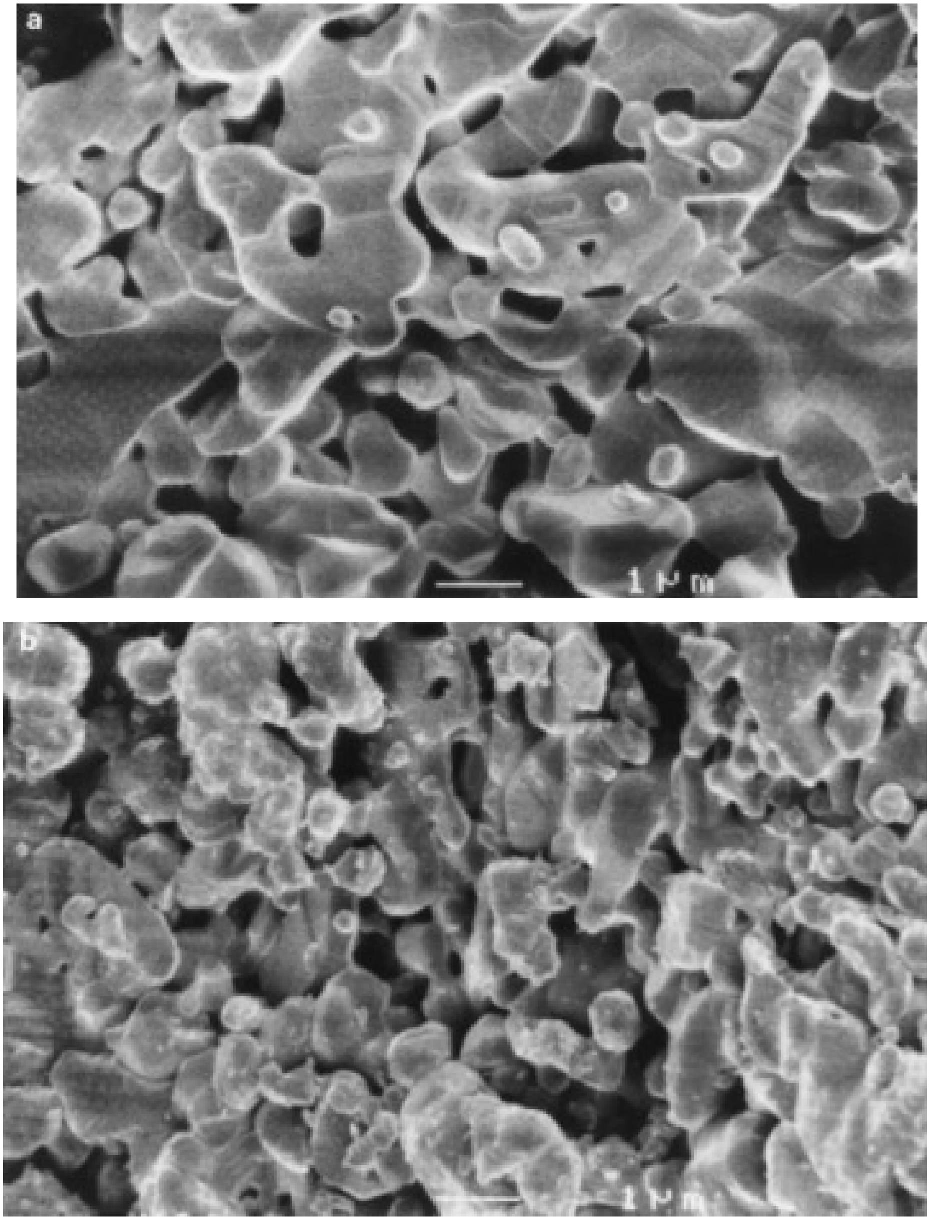

FIG. 1. SEM micrographs obtained from (a) the α-alumina support and (b) the Cs-promoted Ag/α-Al$_2$O$_3$ catalyst.

mostly covered with silver. The assertion that the coating is quite uniform is consistent with the EDS data presented in Table 1. These data were taken from both the support and the catalyst at two different points on each sample. The points were selected to give a maximum compositional difference based on differences in appearance in the SEM micrographs. The compositions determined for the two points on each sample are not very different indicating that both the support and catalyst have fairly uniform near-surface compositions.

ISS

ISS is one of the most important techniques for studying catalysts because it probes only the outermost atomic layer which is the region of greatest importance in catalysis. ISS data obtained from α-alumina and the Cs-promoted, Ag/α-Al$_2$O$_3$ catalyst are shown in Figs. 2a and 2b, respectively. The spectrum obtained from α-alumina exhibits a predominant O feature near an E/E_0 of 0.4. Features are also present due to C, N, Na, Al, Si, Ca, and Ni. Of these the Na and Si are added to the α-alumina as binder materials and the C, N, Ca, and Ni are impurities. The C and Ca are often observed as impurities on oxide surfaces, and the origin of the Ni is not known. The Ag peak is the predominant feature in the ISS spectrum obtained from the catalyst. Small features due to O and Al are also apparent in this spectrum. In a previous ISS calibration study (16), the O/Ag sensitivity ratio was found to be about 0.05

TABLE 1

Composition (wt%) from EDS Data

	Al	O	Ag
Support	55	45	—
	62	38	—
Catalyst	21	25	54
	25	31	44

under the same conditions as those used in this present study. Since the ISS sensitivity is an increasing function with mass, the sensitivity factor of Al would lie between those of O and Ag. The relative peak areas and the sensitivity factors suggest that roughly 50% of this surface consists of O which is associated with both Ag and Al as discussed below. Based on results from the previous study, Ag is about 50% covered with O after heating at 250°C in 200 Torr of O_2 for 1 h. Assuming that this case is similar implies that the Ag almost completely covers the alumina surface. This is consistent with the amounts of Ag and alumina apparent in the SEM micrograph shown in Fig. 1b. Other small features are present due to Na, S, Cl, Ca, and Ni. Most of these are present on the support except for S which accumulates on the Ag with exposure to air. A peak or shoulder due to Cs is not apparent at the high E/E_0 side of the Ag peak indicating that Cs is not present in the outermost atomic layer.

AES

Auger spectra obtained from the α-alumina support and the Cs-promoted, Ag/α-Al_2O_3 catalyst are shown in Figs. 3a and 3b, respectively. The spectrum taken from α-alumina is typical of Auger spectra obtained from alumina surfaces with regard to the Al and O peak sizes, positions and shapes (17). Small features are also present due to the Si and Na (not shown) binder and contaminants including S, Cl, and Ca, which were all identified in the corresponding ISS spectrum.

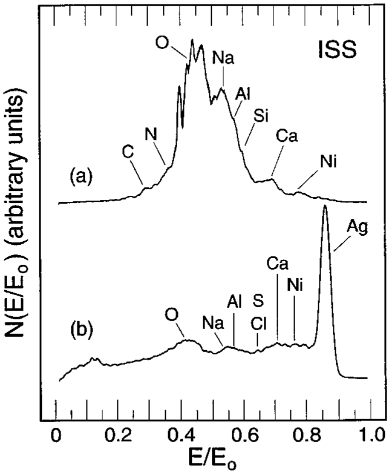

FIG. 2. ISS spectra obtained from (a) the α-alumina support and (b) the Cs-promoted Ag/α-Al_2O_3 catalyst.

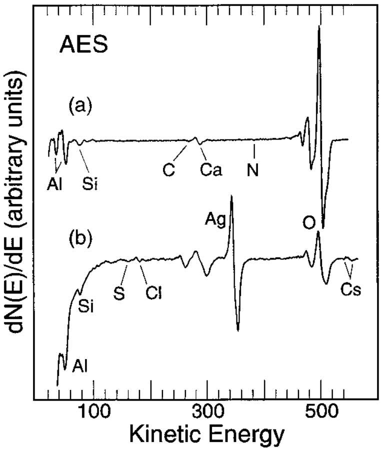

FIG. 3. Auger spectra obtained from (a) the α-alumina support and (b) the Cs-promoted Ag/α-Al_2O_3 catalyst.

The Auger spectrum obtained from the catalyst exhibits a predominant Ag peak, and the Al and O peaks are much smaller because the Ag covers the α-alumina support. The SEM micrograph from the catalyst surface clearly demonstrates that this near-surface region is not homogeneous so it is not appropriate to calculate the surface composition using the homogeneous assumption (12). Generally, catalyst surfaces are highly nonhomogeneous with complex morphologies which change with history. This means that it is inappropriate to quantify AES and XPS data based on the homogeneous assumption. Worse yet, no methods are available for taking these complex matrix effects into account. Since matrix effects dominate, quantification of AES and XPS data obtained from catalyst surfaces is not currently possible. However, qualitative arguments can be made about the composition of the near-surface region of catalysts if morphology is considered. Peaks due to Si, S, Cl, and Cs are also apparent in Fig. 3b. The Cs peaks arise from subsurface Cs illustrating the low surface sensitivity of AES. The results of a calculation of the contribution of subsurface layers to the collected Auger signal for silver has been presented in a previous study (16). About 8% comes from the outermost atomic layer, and about 1% comes from the 30th layer beneath the surface. Therefore, the AES depth distribution profile is very low and broad. This implies that care must be taken in attempting to relate catalytic behavior and results of AES or XPS characterization studies.

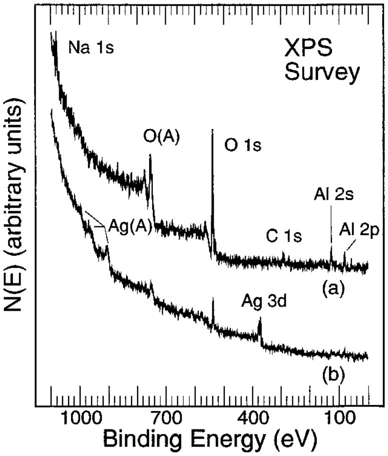

FIG. 4. XPS survey spectra obtained from (a) the α-alumina support and (b) the Cs-promoted Ag/α-Al$_2$O$_3$ catalyst.

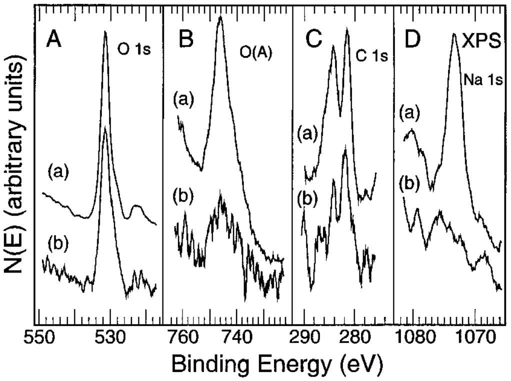

FIG. 6. XPS (A) O 1*s*, (B) O Auger, (C) C 1*s*, and (D) Na 1*s* features obtained from the (a) α-alumina support and (b) Cs-promoted Ag/α-Al$_2$O$_3$ catalyst.

XPS

XPS survey spectra obtained from the α-alumina support and the catalyst are shown in Figs. 4a and 4b, respectively. The spectrum shown in Fig. 4a is typical of survey spectra obtained from alumina except for the large Na 1*s* peak, which originates from the clay binder added to the support. A small Ni 2*p* feature is present at 855.5 eV in a narrow-range spectrum which is consistent with the presence of Ni in the ISS spectrum. As expected, coverage of the α-alumina support by Ag results in reduction of the O, Al, Na, C, and Ni peaks and appearance of Ag Auger, Ag 3*p*, Ag 3*d*, and Ag valence features.

The Al 2*s* and 2*p* peaks obtained from the support and catalyst are shown in Figs. 5a and 5b, respectively. The predominant portions of both peaks correspond to those of Al$_2$O$_3$, but there are also shoulders on the low binding energy sides of both peaks in both spectra. The shoulders are small in Fig. 5a, and they probably arise from an interaction with the Na binder which is present in a significant amount based on the size of the Na 1*s* peak in the corresponding survey spectrum or to Al in Al$_4$C$_3$ as discussed below. A Si 2*p* peak must be present near 100 eV based on the presence of Si in both the ISS and AES spectra, but unlike the Na it is below the noise level. The Na apparently becomes preferentially enriched at the surface during the preparation of the α-alumina. Although the Al 2*s* and 2*p* features obtained from the catalyst are smaller, as is the Na 1*s* feature, the low BE shoulders are relatively larger compared to the predominant features due to Al$_2$O$_3$. This may be due to an electronic (chemical) interaction between the alumina and silver which may be responsible for the differences in catalytic behavior between silver powder and alumina-supported silver. A small feature is also present at about 100 eV which may be due to Si, but again it is within the noise level.

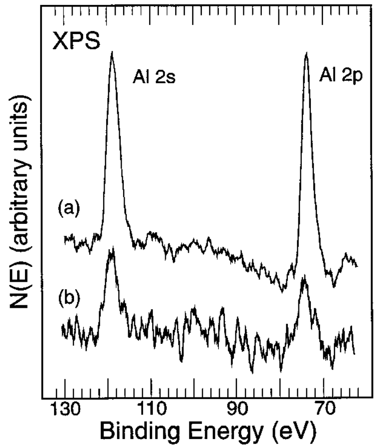

FIG. 5. XPS Al 2*s* and 2*p* spectra obtained from (a) the α-alumina support and (b) the Cs-promoted Ag/α-Al$_2$O$_3$ catalyst.

O 1*s*, O Auger, C 1*s*, and Na 1*s* features obtained from the (a) α-alumina support and (b) catalyst are shown in Figs. 6A, 6B, 6C, and 6D, respectively. The predominant O 1*s* feature obtained from the α-alumina support has a BE of 531.6 eV, which is characteristic of O in Al$_2$O$_3$ (18). There is also a low BE shoulder estimated to lie at 528.2 eV. This shoulder may be due to O associated with Na in some manner and also with the Al responsible for the low BE shoulders on the Al 2*s* and 2*p* peaks. The Na 1*s* peak shown in Fig. 6C, part (a), is broad with a complex shape indicating that more than one chemical state of Na is present. The C 1*s* feature in Fig. 6D, part (a), exhibits two well-defined peaks. The higher BE feature at 284.6 eV is characteristic of adsorbed hydrocarbons which accumulates on most air-exposed samples, and the lower BE feature is characteristic of a carbide such as Al$_4$C$_3$.

Although the predominant O 1*s* feature obtained from the catalyst has a BE of 531.6 eV characteristic of O in

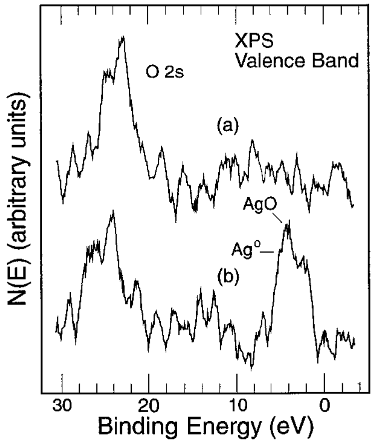

FIG. 7. XPS valence band and O 2*s* features obtained from (a) the α-alumina support and (b) the Cs-promoted Ag/α-Al_2O_3 catalyst.

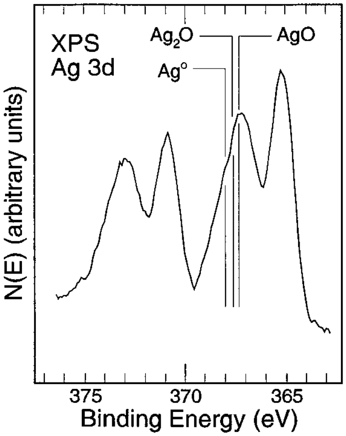

FIG. 8. XPS Ag 3*d* obtained from the Cs-promoted Ag/α-Al_2O_3 catalyst.

Al_2O_3, its shape is different than that obtained from α-alumina. This difference consists mostly of a relative increase in intensity on the low BE portion of the O 1*s* feature. Since the Ag covers the surface, the support O lying more deeply beneath the surface is not observed to the same extent as for the bare surface due to mean-free-path arguments. Therefore, more of the oxygen observed in Figure 6Ab is associated with or influenced by the Ag; i.e., it lies at the α-alumina/Ag interface or in the near-surface region of the Ag. This O apparently has a BE lower than O in Al_2O_3 at 531.6 eV. Some of this O is in the form of AgO and Ag_2O which have BEs of 528.5 and 528.8 eV, respectively (19, 20). The O Auger feature is similarly reduced in size and small Cs features at about the noise level are apparent between 730 and 740 eV. Not only is the Na 1*s* peak reduced in size, but also its shape is quite significantly changed. Three smaller peaks are still apparent at 1071.7, 1075.7, and 1077.0 eV, but the previously predominant feature at 1073.3 eV is absent. The chemical nature of this Na and its disappearance is not understood. Perhaps a volatile Na species sublimes during the calcining step. The C 1*s* feature is similar to that obtained from the α-alumina support, but the peak due to hydrocarbons is reduced compared to the peak at 282.0 eV. Another peak is also apparent at 287.0 eV. This peak is due to the presence of Ag carbonate (or perhaps bicarbonate) which accumulates on the Ag surface during air exposure (19, 20).

The valence band and O 2*s* features obtained from the support and catalyst are shown in Figs. 7a and 7b, respectively. The O 2*s* features from both spectra have similar but complex shapes indicating the presence of multiple forms of O, which is consistent with the O 1*s* data. High-lying core levels such as the O 2*s* often are more sensitive to chemical state than more strongly bound core levels. The valence region provides sensitive information about the chemical state of the Ag. Note that there are no features in this region of the spectrum obtained from α-alumina. This is due to the facts that the cross section for photoemission of valence electrons from oxides using X rays is very small and that the counting conditions used in this study were not sufficient to detect these features. However, the cross section is much larger for photoemission from Ag in the catalyst so distinct valence-band features appear in Fig. 7b. This is of interest because comparison with valence-band features from Ag metal, Ag_2O, and AgO provide Ag chemical-state information. A shoulder at 5.0 eV is apparent, and the peak maximum near 4.5 eV and the small shoulder near the Fermi level are characteristic of AgO (19, 20). Therefore, this valence structure is due to the presence of a mixture of Ag chemical states with an added electronic influence due to the interaction with the alumina support. Since metallic Ag is not very active compared to alumina-supported Ag, the support–metal interaction is very important in determining the catalytic behavior of supported Ag.

The XPS Ag 3*d* peaks obtained from the catalyst surface is shown in Fig. 8. The XPS Ag $3d_{5/2}$ BEs for Ag metal, Ag_2O and AgO are 368.0, 367.7, and 367.3 eV, respectively (19, 20). Based on these assignments, the predominant feature is due to AgO, which is consistent with the valence-band data. However, the peak is broad and subtle shoulders due to Ag_2O and Ag metal are also present. A set of narrow peaks due to charging of one Ag state appear at lower BEs. These are neglected in the Ag 3*d* analysis because they are sufficiently separated from the chemically meaningful Ag 3*d* peaks.

SUMMARY

An α-alumina support material and an as-prepared, Cs-promoted Ag/α-Al_2O_3 ethylene-epoxidation catalyst have been characterized using SEM, EDS, ISS, AES, and XPS. The α-alumina has a crystalline structure with a well-defined flat surface plane exposed according to SEM. Peaks due to the Na and Si added to the alumina (0.4% by weight) as binder materials are observed in the ISS, AES, and XPS spectra, as are small features due to contaminants such as C, N, S, Cl, Ca, and Ni. The XPS spectra are nearly identical to those obtained from pure alumina except for small differences ascribed to interaction of the Al_2O_3 with the Na binder and/or contaminants.

SEM indicates that the Ag fairly uniformly covers most of the α-alumina surface as a thin film. The Ag features are predominant in both the ISS and AES spectra, but alumina, binder, and contaminant features are also apparent. The XPS peak shapes are generally complex due to the presence of multiple chemical states of Ag, Al, O, C, and Na. The shapes and positions of the XPS Ag 3*d* peaks and the valence band structure indicate that AgO, Ag_2O, and Ag metal are all present in significant amounts. The XPS data suggest that there is an electronic interaction between the Ag and the alumina, but the nature of this interaction is not understood. This interaction may be at least partially responsible for the differences in catalytic behavior of Ag metal and alumina-supported Ag.

ACKNOWLEDGMENTS

Financial support for this research was provided by the National Science Foundation through Grant CTS-9122575. The assistance of William S. Epling is appreciated with regard to manuscript preparation and technical comments. The scanning electron micrographs and EDS data were obtained by Phil Tate.

REFERENCES

1. *C&E News*, Apr. 10, 1995, p. 17.
2. Lefort, T. E. (to Societe Francaise de Catalyse Generalisee), Fr. Pat. 729,952, March 27, 1931 and subsequent additions.
3. Nielsen, R. P., and LaRochelle, J. H., U.S. Patent 4 012 425 (1977).
4. Satterfield, C. N., "Heterogeneous Catalysis in Industrial Practice," 2nd ed., p. 279. McGraw–Hill, New York, 1991.
5. Van Santen, R. A., and Kuipers, H. P. C. E., *Adv. Catal.* **35,** 265 (1987).
6. Hoflund, G. B., and Minahan, D. M., submitted for publication.
7. Miller, A. C., *in* "Treatise on Analytical Chemistry" (J. D. Winefordner, Ed.), 2nd ed., Vol. 11, Part 1, Chap. 5, p. 253. Wiley, New York, 1989.
8. Young, V. Y., and Hoflund, G. B., *Anal. Chem.* **60,** 269 (1988).
9. Young, V. Y., Hoflund, G. B., and Miller, A. C., *Surf. Sci.* **235,** 60 (1990).
10. Melendez, O., Hoflund, G. B., Gilbert, R. E., and Young, V. Y., *Surf. Sci.* **251–252,** 228 (1991).
11. Young, V. Y., Welcome, N., and Hoflund, G. B., *Phys. Rev. B* **48,** 2981 (1993).
12. Hoflund, G. B., Asbury, D. A., Corallo, C. F., and Corallo, G. R., *J. Vac. Sci. Technol. A* **6,** 70 (1988).
13. Bhasin, M. M., Ellgen, P. C., and Hendrix, C. D., U.S. Patent 4 916 243 (1990).
14. Gilbert, R. E., Cox, D. F., and Hoflund, G. B., *Rev. Sci. Instrum.* **53,** 1281 (1982).
15. Savitzky, A., and Golay, M. J. E., *Anal. Chem.* **36,** 1627 (1964).
16. Davidson, M. R., Hoflund, G. B., and Outlaw, R. A., *J. Vac. Sci. Technol. A* **9,** 1344 (1991).
17. Davis, L. E., MacDonald, N. C., Palmberg, P. W., Riach, G. E., and Weber, R. E., "Handbook of Auger Electron Spectroscopy." Physical Electronics Division, Perkin–Elmer Corp., Eden Prairie, MN, 1976.
18. Wagner, C. D., Riggs, W. M., Davis, L. E., Moulder, J. F., and Muilenberg G. E., (Eds.), "Handbook of X-Ray Photoelectron Spectroscopy." Physical Electronics Division, Perkin–Elmer Corp., Eden Prairie, MN, 1979.
19. Weaver, J. F., and Hoflund, G. B., *J. Phys. Chem.* **98,** 8519 (1994).
20. Weaver, J. F., and Hoflund, G. B., *Chem. Mater.* **6,** 1693 (1994).